

A Double-Tailed Fluorescent Surfactant with a Hexavanadate Cluster as the Head Group**

Panchao Yin, Pingfan Wu, Zicheng Xiao, Dong Li, Emily Bitterlich, Jin Zhang, Peng Cheng, Dmitri V. Vezenov, Tianbo Liu,* and Yongge Wei*

Surfactants are common amphiphilic materials that usually contain small polar head groups and long hydrophobic tails. Surfactants can self-assemble into micellar or vesicular structures in both polar and nonpolar media (in this case the assemblies are referred as reverse micelles or reverse vesicles) and consequently create microenvironments.^[1] Recently, some novel surfactants with large inorganic metal oxide clusters as polar head groups have been synthesized.^[2–4] The metal oxides are mostly polyoxometalates (POMs), a large class of polyanionic, relatively hydrophilic clusters that consist of early transition metals (usually Mo, W, V, Nb, and Ta) in their highest oxidation states and oxo ligands.^[5,6] Grafting hydrophobic components to the clusters can introduce amphiphilic properties to the POMs and enhances the compatibility of POM clusters with nonpolar media, which will expand the potential applications of these clusters.^[1] For example, Cronin and co-workers succeeded in covalently linking two alkyl chains to both sides of Anderson-type POMs,^[2] and we have demonstrated the formation of regular vesicles and reverse vesicles in different solvents.^[7] Polarz and co-workers functionalized Keggin-type POMs with two alkyl chains and then studied the emulsification properties and counterion-dependent self-assembly behavior of the resulting compounds in solution.^[3] These POM-based surfactants are

unique because 1) they have multifunctional POM polar head groups with applications in catalysis, medicine, and materials science^[2–4] and 2) the POM head groups have adjustable size, shape, and charge, which might lead to adjustable and controllable self-assembly since their packing parameter P_s should be different from those of common surfactants.^[2–4]

Among polyoxovanadates (POVs), hexavanadate clusters have gained increasing interest in recent years because of their nanoscale superoctahedral cluster-core structures, fascinating electronic and magnetic properties, various thermodynamically stable redox isomers, and potential catalytic capabilities.^[8] Zubietta and co-workers made early contributions by synthesizing $[V_6O_{13}H_x\{(OCH_2)_3CR\}_2]^{n-}$ ($x, n = 0, 2; 2, 0; 4, 2; 6, 2; R = NO_2, CH_2OH, CH_3$) with the help of trisalkoxo μ -bridging tripodal ligands, and studied their redox properties.^[9] These compounds can be functionalized with carboxylic groups and used to further develop metal–organic frameworks (MOFs) through coordination bonds with metal ions. The MOF with the $[V_6O_{13}H_x\{(OCH_2)_3CR\}_2]^{n-}$ backbone is well known for its ordered nanoscale porous structure and large inner surface area, and displays high heterogeneous catalytic activity, as confirmed by Hill and co-workers.^[10]

Herein, we report an approach to synthesizing a novel hexavanadate–organic hybrid molecule, $[V_6O_{13}\{(OCH_2)_3CCH_2OOC(CH_2)_{16}CH_3\}_2]^{2-}$ (**1**), and use its amphiphilic properties to enhance their compatibility in both hydrophobic and hydrophilic phases. Two C_{18} alkyl chains were grafted onto two opposite sides of the hexavanadate cluster by the esterification reaction between stearic acid and $((C_4H_9)_4N)_2[V_6O_{13}\{(OCH_2)_3CCH_2OH\}_2]$ (Figure 1). An unexpected blue luminescence from the inorganic clusters was observed when the tetrabutylammonium (TBA) counterions were replaced by protons to give, to the best of our knowledge, the first POM-based compound with counterion-dependent fluorescent properties. More importantly, solvent polarity and the counterion-effect-directed adaptable amphi-

[*] P. Yin,^[†] P. Wu,^[†] Dr. Z. Xiao,^[†] Dr. J. Zhang, Prof. Y. Wei

Department of Chemistry, Tsinghua University

Beijing 100084 (P. R. China)

Phone: 86-10-62797852

Fax: 86-10-62771149

E-mail: yonggewei@mail.tsinghua.edu.cn

P. Yin,^[†] D. Li, E. Bitterlich, P. Cheng, Prof. D. V. Vezenov, Prof. T. Liu

Department of Chemistry, Lehigh University

6 E Packer Avenue, Bethlehem

PA 18015 (USA)

Fax: 1-610-758-2935

E-mail: liu@lehigh.edu

Homepage: <http://www.lehigh.edu/~inliu>

P. Wu^[†]

School of Chemical & Environmental Engineering

Hubei University of Technology, Wuhan 430068 (China)

[†] These authors contributed equally to this work.

[**] This work is supported by NFSC nos. 91022010, 20871073, and 20921001, THSJZ, and Tsinghua University Initiative Foundation Research Program no. 20101081771. T.L. acknowledges support from NSF CHM0545983 and Alfred P. Sloan Foundation. P.W. acknowledges support from the Foundation of Educational Commission of Hubei Province (no. B200614006) and the Natural Science Foundation of Hubei Province (no. 2008CDB020).

Supporting information for this article is available on the WWW under <http://dx.doi.org/10.1002/anie.201006144>.

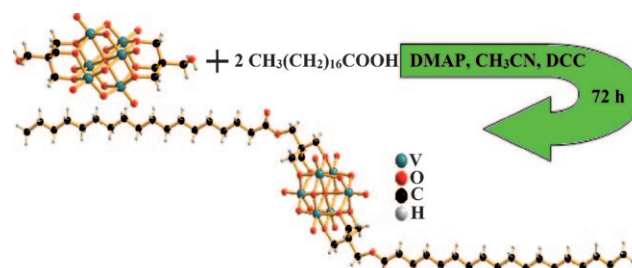


Figure 1. Synthesis of **1**²⁻. DCC = 1,3-dicyclohexylcarbodiimide, DMAP = 4-dimethylaminopyridine.

philic nature of **1** were exhibited through its self-assembly behavior that was studied with various counterions and in different solvents by using light scattering, ^1H NMR, SEM, and TEM techniques.

Platelike single crystals of $\text{TBA}_2\mathbf{1}$ were obtained after attempting different crystallization strategies. Although the X-ray diffraction intensities at high angles are very weak because of the rather small thickness of the crystals, the locations of all the atoms can be determined very accurately, which is rare for compounds that contain such long alkyl chains. The space group of $\text{TBA}_2\mathbf{1}$ is $P\bar{1}$ and there is an inversion center located at the central oxygen atom of the hexavanadate cluster in **1**. The POV cluster anion can be treated as a cluster consisting of two $[\text{RC}(\text{CH}_2\text{O})_3]^{3-}$ subunits bound to a $[\text{V}_6\text{O}_{13}]^{4+}$ core, or, alternatively, a hexametalate $[\text{V}_6\text{O}_{19}]^{8-}$ core connected to two $[\text{RC}(\text{CH}_2)_3]^{3+}$ subunits. The trisalkoxy ligands occupy opposite faces of the hexametalate octahedron. The conformation of the long alkyl tails in crystals is close to the ideal zig-zag shape, which favors the parallel stacking of chains. The length of a single chain is approximately 2.48 nm in the crystalline state, whilst the size of the polar head is approximately 0.76 nm, which is much larger than the sulfate group (ca. 0.20 nm), which is the polar head of a common ionic surfactant sodium dodecyl sulfate (SDS). Differential scanning calorimetry (DSC) and thermogravimetric analysis (TGA) results indicate that the melting temperature of $\text{TBA}_2\mathbf{1}$ is 95.15 °C and the decomposition temperature is as high as 250 °C (Figures S1 and S2 in the Supporting Information).

In the packing diagram (Figure 2, left), the *ab* plane (the (001) lattice plane) was formed because of the close packing of the TBA ion and the hexavanadate cluster. The area between two neighboring lattice planes is filled by the alkyl chains (interplane distance: 1.88 nm). The nonpolar tails tend to align side-by-side in order to strengthen the van der Waals interactions between them, which is much weaker than the ionic interactions in the *ab* plane. The structural analysis indicates that the driving force for the crystal growth is anisotropic. As a result, the growth along the (001) lattice plane direction to form thin plate-shaped crystals is favored.

The TBA counterions can be replaced by protons and thus $\text{H}_2\mathbf{1}$ was obtained by using cation-exchange resin. ^1H NMR spectroscopy confirmed that all the TBA ions were replaced and the hydrogen atoms in the organic part of **1** remained

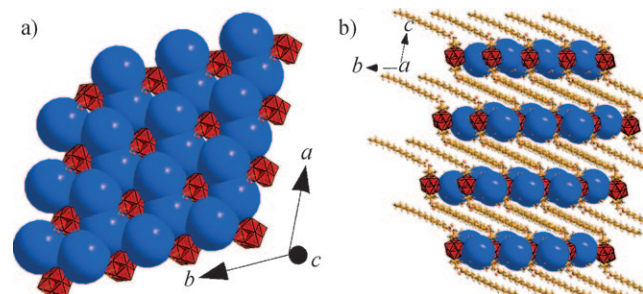


Figure 2. Packing diagram of $\text{TBA}_2\mathbf{1}$. a) *ab* plane or (001) lattice plane; b) *bc* plane or (100) lattice plane. Blue spheres represent TBA ions and red polyhedra represent hexavanadate clusters.

after cation exchange. $\text{V}-\text{O}_\text{t}$, $\text{V}-\text{O}_\text{b}$, $\text{C}-\text{O}$, and $\text{C}=\text{O}$ vibrations were visible in the IR spectrum of $\text{H}_2\mathbf{1}$ (O_t , terminal oxo and O_b , bridge oxo; Figures S3 and S4). The pH value of the saturated aqueous solution of $\text{H}_2\mathbf{1}$ is 2.75. In addition, $\text{Na}_2\mathbf{1}$ was synthesized by titrating the saturated solution of $\text{H}_2\mathbf{1}$ to pH 7 with NaOH solution.

Interestingly, $\text{H}_2\mathbf{1}$ shows strong blue luminescence in both aqueous and acetone solutions. Both $\text{H}_2\mathbf{1}$ and $\text{Na}_2\mathbf{1}$ emit blue luminescence with peaks at 392 nm, 409 nm, and 429 nm (Figure 3a,b). The luminescence spectra from both solutions are similar. The major difference is that the intensities of the

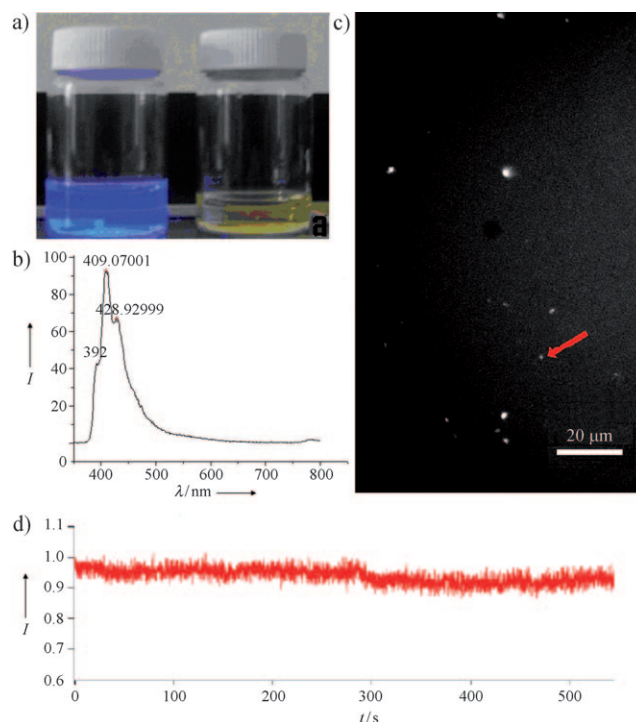


Figure 3. a) $\text{H}_2\mathbf{1}$ (left; in aqueous solution) and $\text{TBA}_2\mathbf{1}$ (right; in acetonitrile) solutions under UV light. b) Luminescence spectrum of $\text{H}_2\mathbf{1}$ excited at 335 nm. c) Luminescence image of $\text{H}_2\mathbf{1}$ in aqueous solution. d) Normalized intensity changes over time for the dot marked with the red arrow in (c), thus demonstrating the stability of the blue luminescence of **1**.

first and the third peaks are higher than that of the second peak for the $\text{Na}_2\mathbf{1}$ solution whilst for the $\text{H}_2\mathbf{1}$ solution the opposite situation is observed (Figure S8). Excitation with light of wavelengths between 300–420 nm can trigger such blue luminescence. No emission is observed if the wavelength of the light is below 300 nm. The excitation band for $\text{H}_2\mathbf{1}$ is around its ligand-to-metal (LMCT) charge transfer (oxo–vanadium) absorption wavelength, and it is possible that the origin of the emission involves an emissive state derived from an LMCT transition.^[11]

Several other POMs were also found to have photoluminescent properties in the solid state at very low temperatures (e.g., 4 K). A few of these compounds retain this property in aqueous solution at room temperature.^[12] The photoluminescence mainly comes from the introduction of

Eu³⁺ ions; most POMs without Eu³⁺ ions are not luminescent, and, furthermore, they are usually considered as luminescence quenchers because of their special ability to store electrons and stabilize fragile structures.^[13] Hong and co-workers, who claimed that luminescent properties have rarely been reported for vanadium oxide clusters, observed that (Et₄N)₅[V₁₄O₃₆Cl] produces intense blue luminescence in aqueous solution.^[11]

To further understand the luminescent properties of **1**, the luminescence of [V₆O₁₃((OCH₂)₃COH)₂]²⁻ was investigated with different counterions. The same luminescence signal with a much lower intensity was observed in the case of H₂**1**. Zubietta and co-workers showed that a minor structural change was observed in the [V₆O₁₃((OCH₂)₃CR)₂] (R = NO₂, CH₂OH, CH₃) core when the protons associated with the bridge oxygen ligands.^[9] This change might also lead to the red-shift of the characteristic peak from 350 nm (TBA₂**1**) to 369 nm (H₂**1**) in the UV/Vis spectrum. It is possible that the structural change of the POV cores after counterion exchange leads to luminescence.^[9] Moreover, the self-assembly of **1** and the presence of protons or Na⁺ ions as counterions probably results in the higher luminescence intensity of **1**. The distances between the polar head groups should be very small because of the small sizes of protons and Na⁺ ions in the assemblies and the interaction between the POV polar head groups would become much stronger, which may increase the luminescence intensity.

When excited at 410 nm, the aggregates of H₂**1** in aqueous solution can be observed by fluorescence microscopy (Figure 3c,d) as very tiny (diffraction-limited size) dots. The intensity of a selected dot (Figure 3c) did not show obvious decay over 30 minutes, which is very different from the behavior of organic fluorophores that exhibit photobleaching, and confirms that the polyvanadate hybrid does not decompose under UV irradiation. Another possibility is that the alkyl tails might be cleaved from the POV while the head group remains intact. This process can be ruled out based on our detailed studies on the self-assembly of these hybrids, as the large assemblies (the microspheres observed under the fluorescence microscope) will not be stable after loss of the alkyl chains. The possible connections between the luminescence properties and solution behavior of the hybrid compounds led us to explore their self-assembly in solution.

Compound TBA₂**1** is soluble in polar organic solvents such as acetone, acetonitrile, DMF, and DMSO, but not soluble in nonpolar organic solvents or water. The electrostatic interaction between the TBA groups and POVs, and the hydrophobic interaction between the alkyl chains on the TBA groups and the organic ligands on the hybrids will have simultaneous roles in solution, thus leading to a very complicated situation.

The diffusion coefficients of **1**²⁻ and the TBA ions obtained from DOSY ¹H NMR spectroscopy experiments were used to characterize the interaction between the TBA ions and POVs in solution (Table S1). When TBA₂**1** is dissolved in acetone, the diffusion coefficient *D* of the TBA ions is a little lower than that in tetrabutylammonium iodide (TBAI), but quite close to the diffusion coefficient of the hybrid anions. However, when water was added to the

solution (volume fraction from 1/9 to 1/3), the *D* value of TBA ions is nearly the same as that of TBAI and interestingly, much larger than the *D* values of the hybrids in the same solution (see the Supporting Information). These results suggest that the disassociation of TBA counterions from POVs becomes more significant when the solvent becomes more polar. Compared to the water/acetone mixtures, the TBA ions associate very closely with the hexavanadate surface in acetone solution because of the low dielectric constant of the solvent, that is, water can promote the dissociation of TBA ions from the hexavanadate clusters and increase the net charge on the POVs. Consequently, the POV part becomes more hydrophilic and the overall hybrid molecule becomes amphiphilic in nature, thus resulting in possible self-assembly behavior in solution (Figure 4). This speculation is confirmed by our results from light scattering experiments, since the scattered light intensity from the solution of TBA₂**1** increased significantly and large vesicles were observed when 20–35 % of water (by volume) was added to a solution of TBA₂**1** in acetone. When the solvent contains up to 12.5 % of water, the scattered intensity was pretty low (39.1 kcps), thus suggesting that no supramolecular structure

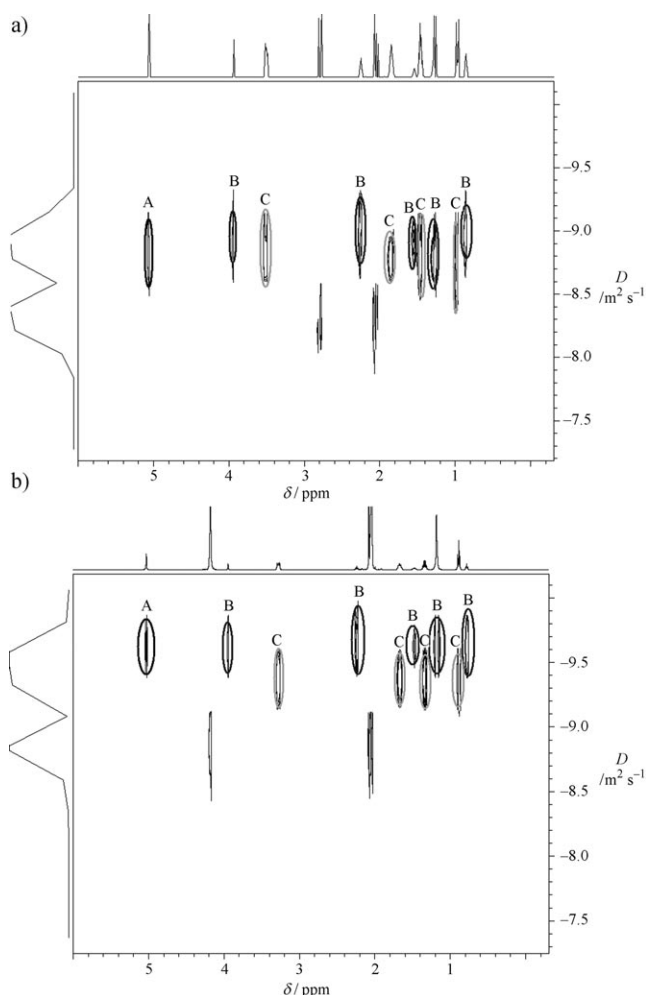


Figure 4. DOSY spectra for solutions of TBA₂**1** a) in acetone and b) in water/acetone (1:3). A = signal for POV head, B = signal for tail, C = signal for TBA ion, the remaining signals arise from the solvent.

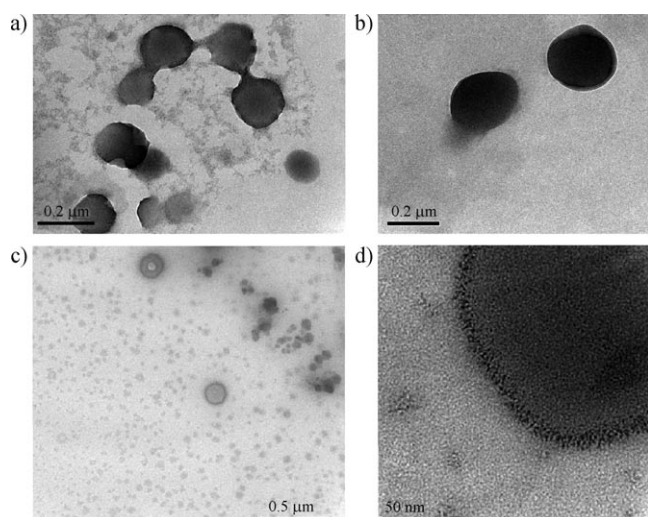


Figure 5. TEM images of the vesicles formed in a) 0.6 mg mL^{-1} $\text{TBA}_2\mathbf{1}$ in water/acetone (1:4), b) 0.75 mg mL^{-1} $\text{TBA}_2\mathbf{1}$ in water/acetone (1:3), and c) $\text{Na}_2\mathbf{1}$ in aqueous solution. d) Expansion of image in (c).

was formed. Vesicles were observed when the proportion of water in the solvent mixture is over 20%, as confirmed by TEM studies (Figure 5a,b). As more and more water was added, the vesicle size became larger and larger (Table S2). A possible reason for this behavior is that when the polarity of the solvent increases, the interaction between the alkyl chains and the solvent molecules becomes less favorable and the chains will stack closer to lead to a smaller curvature, that is, a spherical structure will have a larger size. The solution became cloudy when 35 vol% of water was added. SEM studies indicate that plate-shaped microcrystals exist in the cloudy suspension. All the plates are very uniform in size with a thickness of $1.8 \mu\text{m}$ (see Figure 6). Compound $\text{TBA}_2\mathbf{1}$ can be

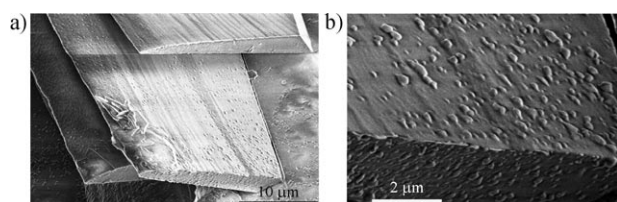


Figure 6. a) SEM image of microsheet structure formed by $\text{TBA}_2\mathbf{1}$. b) Expansion of the microsheet surface.

considered as a special short-chain polymer. Amorphous materials will usually be obtained when polymers experience a sudden change from a solvent in which they are soluble to one in which they are insoluble. It is possible that the observed microsheet structures arise from the collapse and layered packing of vesicles in the solution.

The vesicle size is less dependent on the concentration of $\text{TBA}_2\mathbf{1}$. In a water/acetone mixture (1:4), the average vesicle radius was around 180–220 nm for concentrations from 0.375 to less than 1.5 mg mL^{-1} . SEM results indicate that the cloudy solution observed at 1.5 mg mL^{-1} contains similar microplate crystals described above.

The dissociation of TBA ions from POVs and the vesicle formation are clearly correlated, according to the zeta potential analysis. As the water content is increased, the zeta potential value of the hybrids becomes more negative, and leads firstly to the vesicle formation and then gradually larger vesicles. For the solutions with the same water content, the zeta potential values are quite close to each other (Table S2) at different hybrid concentrations.

Recently, we have shown the self-assembly of hybrid Anderson clusters grafted with two alkyl chains (**2**; see the Supporting Information) into bilayer vesicles.^[7] The addition of water can also trigger the formation of vesicles for **2**, which was not clearly understood in our previous work. The experimental data here clearly correlates the effect of water content with the state of the TBA ions and the formation of aggregates. As a result, the hydrophilicity of the hybrid surfactant is continuously adjustable, which is different from the common surfactants. Interestingly, a much higher water content is needed for hybrid **2** to form vesicles; this behavior could be due to the fact that the Anderson cluster in **2** has a higher charge than the hexavanadate cluster in **1** (−3 vs. −2). The higher charge leads to a stronger attraction between the POMs and TBA ions, thus implying that more water is required for the dissociation process.

When the TBA ions were replaced by protons or Na^+ ions, the resulting compound can be dissolved in water and smaller vesicles (57 nm and 55 nm, respectively) were observed by light scattering studies. The zeta potential of $\text{Na}_2\mathbf{1}$ is -80.6 mV , which is much more negative than that of $\text{TBA}_2\mathbf{1}$ (ca. 50 mV), while $\text{H}_2\mathbf{1}$ shows a less negative value (-30.9 mV), which is probably due to ion pairing or protonation. TEM images also reveal some smaller spherical structures that are possibly some small micelles (see Figure 5c,d).

The vesicle formation process of **1** is different from that of **2**, and is comparatively fast with all types of counterions. A large amount of vesicles with very large sizes are observed within one day. The difference might also be explained by the different negative charges of the POM head groups.

All the experimental results, especially those from NMR studies, show that the driving force of the vesicle formation is the solvent-phobic interaction, which is similar to that of conventional surfactants. The large and rigid structure of the hexavanadate head groups, the conformation frustration of the alkyl chains needed for forming bilayers, and the charge repulsion between the POM head groups on vesicle surface in both **1** and **2** all favor a small curvature and therefore the formation of large vesicles. The relation between the vesicle size of **1** and the dielectric constant of the solvent is opposite to what we have observed in pure POM macroionic solutions where the hydrophilic macroions self-assemble into single-layered vesicle-like blackberry structures because of different driving forces. The size of these structures usually increases as the solvent polarity decreases, thus indicating a charge-regulated process.^[14] The formation of the blackberry structures is driven by the counterion-mediated effect and possibly hydrogen bonding, and not the solvent-phobic interaction.^[14]

The surfactant $\text{Na}_2\mathbf{1}$ can reduce the surface tension of an aqueous solution, thus showing a basic feature of surfactants.

As the concentration increases, the surface tension decreases, and the critical micelle concentration (CMC) is calculated to be 0.23 mg mL^{-1} . The surface tension at the turning point is 45.4 mN m^{-1} , which is much lower than the surface tension of pure water at room temperature (72 mN m^{-1} ; Figure 7).

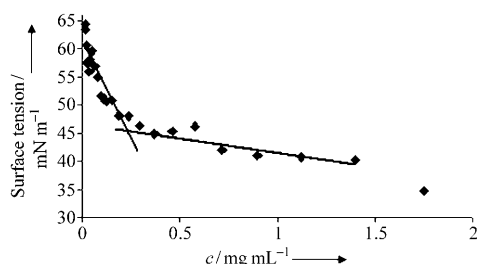


Figure 7. Concentration-dependent surface tension of $\text{Na}_2\mathbf{1}$ (aqueous solution).

In summary, a double-tailed surfactant with a hexavanadate cluster as a polar head group was successfully synthesized and its single-crystal structure, which did not show any disorder, was obtained. Unexpected blue luminescence was observed from the POV core for $\text{H}_2\mathbf{1}$ or $\text{Na}_2\mathbf{1}$. The hybrids demonstrate amphiphilic properties in solution by forming bilayer vesicles, and at the water/air interface by reducing surface tension. These new features might render such hybrids new applications such as enhancing the catalytic properties of POMs in organic media. These compounds might find applications as a fluorescent label because of its broad excitation profile, strong luminescence intensity, and good stability. More importantly, our research might inspire a new mechanism for the generation of fluorescence, as well as to use the controllable self-assembly behavior of the inorganic–organic hybrids to form novel photoactive colloid materials.

Experimental Section

$(\text{TBA})_2[\text{V}_6\text{O}_{13}\{(\text{OCH}_2)_3\text{CCH}_2\text{OH}\}_2]$ was prepared according to previously reported procedures.^[9] $(\text{TBA})_2[\text{V}_6\text{O}_{13}\{(\text{OCH}_2)_3\text{CCH}_2\text{OH}\}_2]$ (1.26 g, 1 mmol), DCC (0.44 g, 2.1 mmol), and stearic acid (1.14 g, 4 mmol) were dissolved in 50 mL acetonitrile. DMAP (0.2 g, 1.6 mmol) was added to the resulting solution. The mixture was stirred at 80°C for 72 h and then filtered. Red thin platelike crystals of $\text{TBA}_2\mathbf{1}$ were collected from the filtrate after two days (0.17 g, 10% yield).

$\text{TBA}_2\mathbf{1}$ $(\text{Bu}_4\text{N})_2[\text{V}_6\text{O}_{13}\{(\text{OCH}_2)_3\text{CCH}_2\text{OOC}(\text{CH}_2)_{16}\text{CH}_3\}_2]$: $^1\text{H NMR}$ (500 MHz, $[\text{D}_6]\text{acetone}$, 300 K): $\delta = 0.8640$ (t, 6H, CH_3 , tail), 0.9745 (t, 24H, CH_3 , $[\text{Bu}_4\text{N}]^+$), 1.2708 (m, 52H, $(\text{CH}_2)_{13}$, tail), 1.4641 (m, 16H, CH_2 , $[\text{Bu}_4\text{N}]^+$), 1.5487 (m, 4H, CH_2 , tail), 1.8425 (m, 16H, CH_2 , $[\text{Bu}_4\text{N}]^+$), 2.2000 (m, 4H, $\text{OOC}-\text{CH}_2$, tail), 3.5113 (t, 16H, NCH_2 , $[\text{Bu}_4\text{N}]^+$), 3.9401 (t, 4H, $\text{COO}-\text{CH}_2$, tail), 5.0630 ppm (s, 12H, $(\text{OCH}_2)_3$); IR (KBr pellet): $\tilde{\nu} = 2961$ (s), 2922 (s), 2872 (s), 2852 (s), 1752 (s), 1485 (m), 1469 (s), 1384 (m), 1159 (m), 1132 (m), 1062 (s), 961 (s), 942 (vs), 881 (w), 812 (m), 720 (s), 582 (m), 513 cm^{-1} (w); UV/Vis (MeCN): $\lambda_{\text{max}} = 350 \text{ nm}$; ESI (MeCN): m/z : 656.35 $[\mathbf{1}^-]$, 1313.22 $[(\mathbf{1} + \text{H})^-]$, 1554.50 $[(\mathbf{1} + \text{TBA})^-]$; elemental analysis calcd (%) for $\text{C}_{78}\text{H}_{158}\text{N}_2\text{O}_{23}\text{V}_6$: C 52.11, H 8.86, N 1.56; found: C 52.14, H 8.80, N 1.61.

Crystal data for $\text{TBA}_2\mathbf{1}$ $\text{C}_{78}\text{H}_{158}\text{N}_2\text{O}_{23}\text{V}_6$: $M_r = 1797.70$, triclinic, $P\bar{1}$, $a = 11.528(2)$, $b = 12.074(2)$, $c = 19.371(4) \text{ \AA}$, $\alpha = 94.67(3)^\circ$, $\beta =$

$99.95(3)^\circ$, $\gamma = 115.39(3)^\circ$, $V = 2362.3(8) \text{ \AA}^3$, $Z = 1$, $\rho_{\text{calcd}} = 1.264 \text{ g cm}^{-3}$, $\mu = 0.634 \text{ mm}^{-1}$, $F(000) = 962.0$, crystal size $= 0.30 \times 0.30 \times 0.05 \text{ mm}^3$. A total of 10660 reflections were collected, of which 4724 were unique ($R_{\text{int}} = 0.1004$). $R_1 = 0.0709$ for 3676 independent reflections with $[I > 2\sigma(I)]$, $wR_2 = 0.1345$ for all data. The data were collected at 298(2) K on a Rigaku R-Axis RAPID IP diffractometer with MoK_α monochromated radiation ($\lambda = 0.71073 \text{ \AA}$). The structures were solved by direct methods using SHELXS-97 and refined using SHELXL-97.^[15] CCDC-805404 contains the supplementary crystallographic data for this paper. These data can be obtained free of charge from the Cambridge Crystallographic Data Centre via www.ccdc.cam.ac.uk/data_request/cif.

Received: October 1, 2010

Revised: December 30, 2010

Published online: February 17, 2011

Keywords: hybrid materials · luminescence · polyoxometalates · self-assembly · surfactants

- a) C. Tanford, *Proc. Natl. Acad. Sci. USA* **1979**, *76*, 4175–4176; b) C. Tanford, *The Hydrophobic Effect*, Wiley Interscience, New York, **1973**.
- Y. F. Song, N. McMillan, D. L. Long, J. Thiel, Y. L. Ding, H. S. Chen, N. Gadegaard, L. Cronin, *Chem. Eur. J.* **2008**, *14*, 2349–2352.
- S. Landsmann, C. Lizandara-Pueyo, S. Polarz, *J. Am. Chem. Soc.* **2010**, *132*, 5315–5321.
- Y. Han, Y. Xiao, Z. Zhang, B. Liu, P. Zheng, S. He, W. Wang, *Macromolecules* **2009**, *42*, 6543–6548.
- D.-L. Long, R. Tsunashima, L. Cronin, *Angew. Chem.* **2010**, *122*, 1780–1803; *Angew. Chem. Int. Ed.* **2010**, *49*, 1736–1758.
- C. L. Hill (Guest Ed.), *Chem. Rev.* **1998**, *98*, 1–389.
- a) J. Zhang, Y.-F. Song, L. Cronin, T. Liu, *J. Am. Chem. Soc.* **2008**, *130*, 14408–14409; b) J. Zhang, Y.-F. Song, L. Cronin, T. Liu, *Chem. Eur. J.* **2010**, *16*, 11320–11324.
- a) C. Daniel, H. Hartl, *J. Am. Chem. Soc.* **2005**, *127*, 13978–13987; b) C. Daniel, H. Hartl, *J. Am. Chem. Soc.* **2009**, *131*, 5101–5114; c) C. Aronica, G. Chastanet, E. Zueva, S. A. Borshch, J. M. Clemente-Juan, D. Luneau, *J. Am. Chem. Soc.* **2008**, *130*, 2365–2371; d) J. Spandl, C. Daniel, I. Brudgam, H. Hartl, *Angew. Chem.* **2003**, *115*, 1195–1198; *Angew. Chem. Int. Ed.* **2003**, *42*, 1163–1166.
- Q. Chen, D. P. Goshorn, C. P. Scholes, X.-I. Tan, J. Zubieta, *J. Am. Chem. Soc.* **1992**, *114*, 4667–4681.
- a) J. W. Han, K. I. Hardcastle, C. L. Hill, *J. Am. Chem. Soc.* **2007**, *129*, 15094–15095; b) J. W. Han, K. I. Hardcastle, C. L. Hill, *Eur. J. Inorg. Chem.* **2006**, 2598–2603.
- L. Chen, F. Jiang, Z. Lin, Y. Zhou, C. Yue, M. Hong, *J. Am. Chem. Soc.* **2005**, *127*, 8588–8589.
- T. Yamase, *Mol. Eng.* **1993**, *3*, 241–254.
- T. M. Anderson, W. A. Neiwert, M. L. Kirk, P. M. B. Piccoli, A. J. Schultz, T. F. Koetzle, D. G. Musaev, K. Morokuma, R. Cao, C. L. Hill, *Science* **2004**, *306*, 2074–2077.
- a) M. Kistler, A. Bhatt, G. Liu, T. Liu, *J. Am. Chem. Soc.* **2007**, *129*, 6453–6454; b) D. Li, J. Zhang, K. Landskron, T. Liu, *J. Am. Chem. Soc.* **2008**, *130*, 4226–4227; c) A. A. Verhoeff, M. L. Kistler, A. Bhatt, J. Pigga, J. Groenewold, M. Klokkenburg, S. Veen, S. Roy, T. Liu, W. K. Kegel, *Phys. Rev. Lett.* **2007**, *99*, 066104.
- G. M. Sheldrick, SHELXTL v. 5.10, Structure Determination Software Suite, Bruker AXS, Madison, Wisconsin (USA), **1998**.